A Simple Ice and Liquid Phase Microphysics Scheme

SUPPLEMENTAL MATERIAL TO

Precipitation and Evolution Sensitivity in Simulated Deep Convective Storms: Comparisons between Liquid-Only and Simple Ice and Liquid Phase Microphysics

MATTHEW. S. GILMORE, JERRY M. STRAKA, AND ERIK N. RASMUSSEN

1. Introduction

This supplemental material summarizes the equations for the simple ice and liquid phase microphysics scheme developed by J. M. Straka. The number of ice and liquid species are identical to Lin et al. (1983; hereafter LFO83) and their fundamental production processes are quite similar. This summary is presented in order to insure reproducibility of our results, synthesize information from various earlier writers, and to reconcile those equations that differ in appearance from LFO83. The reader is referred to LFO83 or Chang (1977) for more detailed explanations regarding the history and motivation behind each process.

Regarding differences between these equations and those presented in LFO83, some are merely cosmetic and can be reconciled with one or two substitutions. However, other equations must be derived from first principles to understand the differences. For example, some of the accretion equations differ because we do not neglect the diameter and terminal fall speed of the monodisperse cloud ice/water distributions. This results in general solutions for accretion that are particularly applicable for schemes with more habits. Also, unlike LFO83, tendencies are written in terms of number concentration rather than intercept parameter for easier application in higher-moment versions of the scheme. A final important difference is that the saturation adjustment procedure is more similar to Tao et al. (1989) than Orville and Kopp (1977).

All variables are defined herein, using SI units, and many of the constants and symbols are the same as in LFO83 (see supplemental appendix). One difference is that all process variables are named with the species experiencing the gain (loss) occurring first (last) in the name. For example, the rate of hail melting is written qrmlh (not qhmlr) since rain experiences the gain. Tensor notation is used when possible. Budgets are presented in supplemental section 4n.

Corresponding author address: Dr. Matthew S. Gilmore, Dept. of Atmospheric Sciences, Univ. of Illinois, 105 S. Gregory St., Urbana, IL, 61801. Email: gilmore@atmos.uiuc.edu.

2. Water conservation equations

Water conservation for each species mixing ratio, q, is expressed in tensor form as

$$\frac{\partial q}{\partial t} = -u_i \frac{\partial q}{\partial x_i} + \frac{\partial}{\partial x_i}\left(K_h \frac{\partial q}{\partial x_i}\right) + \frac{1}{\rho}\frac{\partial}{\partial x_3}\left(\overline{V}\rho q\right) + P, \quad \text{(S1)}$$

where the respective terms on the right-hand side represent advection, diffusion, fallout, and microphysical source/sink processes (also see section 4n). There are six interacting water species: water vapor, cloud water, rainwater, cloud ice, snow, and hail/graupel.

3. Distribution parameters

a. Distribution type, mean diameter, intercept, and number concentration

Rain (r), snow (s), and hail/graupel (h) are defined with a Marshall and Palmer (1948) exponential distribution as follows:

$$n_x(D_x) = n_{ox} \exp\left(-D_x D_{nx}^{-1}\right), \quad \text{(S2)}$$

where $x = r, s,$ or h. The mean diameter, D_{nx}, of such a distribution is simply the inverse of the slope parameter. D_{nx} varies with the species mixing ratio content and is diagnosed as

$$D_{nx} = \left[\rho q_x / \left(\pi \rho_x n_{ox}\right)\right]^{1/4}, \quad \text{(S3)}$$

where $x = r, s,$ or h. The default intercepts for rain, snow, and hail/graupel (n_{or}, n_{os}, n_{oh}) are constants set to 8×10^6, 3×10^6, and 4×10^4 m^{-4}, respectively (LFO83).

The default water densities for rainwater, cloud water, snow, and hail/graupel (ρ_r, ρ_w, ρ_s, ρ_h) are constants set to 1000, 1000, 100, and 900 kg m^{-3}, respectively (similar to LFO83). The user may change some of these particular intercepts and/or ice densities on a case-by-case basis. The total number concentration for the rain, snow, and hail/graupel distributions can be found using

$$N_x = n_{ox} D_{nx}, \tag{S4}$$

where $x = r, s,$ or h. Cloud water has a monodisperse distribution whereby all particles share a common mass, M_w, and diameter, D_w, which are functions of the mixing ratio. The diameter of each cloud droplet is defined as

$$D_w = \left(\frac{M_w}{\rho_w} \frac{6}{\pi} \right)^{1/3}, \tag{S5}$$

where the mass of each cloud droplet defined as

$$M_w = q_w \rho / ccn_w. \tag{S6}$$

The limits imposed on D_w range from 2–100 μm (Pruppacher and Klett 1997). It will be shown that the limits on D_w also impose limits on cloud droplet fall speed. The number concentration of cloud droplets is assumed to be identical to the number concentration of active cloud condensation nuclei. LFO83 assume negligible D_w, however, it is diagnosed here for the accretion equations.

Following Rutledge and Hobbs (1983; hereafter RH83), cloud ice is also monodisperse and the common diameter of hexagonal plate ice crystals is given as

$$D_i = 16.7 M_i^{1/2}, \tag{S7}$$

where M_i is the average mass of each ice crystal defined as

$$M_i = q_i \rho / N_i. \tag{S8}$$

Following LFO83 and RH83, the number concentration of cloud ice, N_i, is assumed to be equal to the number of active ice nuclei, N_{in}. Fletcher (1962) found that N_{in} follows

$$N_{in} = N_{in0} \exp\left[-\beta \left(T - T_0 \right) \right], \tag{S9}$$

where N_{in0} = 0.01 m^{-3} and β = 0.6 K^{-1} are the values used by RH83. We limit D_i to range from 10–3000 μm (Davis and Auer 1974) and N_{in} to range from 1–10^9 m^{-3}. It will be shown that the limits on D_i also impose limits on cloud ice crystal fall speed.

Although LFO83 use equation S9 to compute number concentration, they assume constant M_i and negligible D_i. Alternatively, we diagnose D_i explicitly for use in several of the accretion rate computations.

b. Mass-weighted mean terminal fall speed

The mass-weighted mean fall speed equations for rain, snow, and hail, are identical to those presented in LFO83; they may be written as

$$\overline{V}_r = \frac{a\Gamma(4+b)}{6D_{nr}^b} \left(\frac{\rho_0}{\rho} \right)^{1/2}, \tag{S10}$$

$$\overline{V}_s = \frac{c\Gamma(4+d)}{6D_{ns}^d} \left(\frac{\rho_0}{\rho} \right)^{1/2}, \text{ and} \tag{S11}$$

$$\overline{V}_h = \frac{\Gamma(4.5)}{6D_{nh}^{0.5}} \left(\frac{4g\rho_h}{3C_D \rho} \right)^{1/2}. \tag{S12}$$

A representative drag force coefficient (C_D) is about 0.6 for small to moderate-sized oblate spheroidal hailstones and 1.0 for conical graupel (Pruppacher and Klett 1978, 340–341). Since this ice microphysics scheme predicts graupel and hail in a single category, one must choose a single representative C_D. Here, we recommend that a ρ_h of 600 kg m^{-3} be the upper bound for distributions that are composed of mostly graupel-shaped particles (C_D = 1) with denser particles being comprised of mostly hail-shaped particles (C_D = 0.6). This is how C_D was determined herein.

Unlike LFO83, we do not assume that the monodisperse species have negligible mass-weighted mean fall velocity. Instead the average fall speed for monodisperse cloud water droplets and cloud ice crystals is computed using the average diameters defined earlier. In our simulations, we extrapolated the fall speed relation for rain from Liu and Orville (1969) to cloud droplets: $\overline{V}_w = aD_w{}^b \left(\rho_0 / \rho \right)^{1/2}$. This is a reasonable approximation for the larger cloud water diameters. However observed cloud water droplet fall speeds (Gunn and Kinzer 1949) for diameters below 30 μm are better approximated with Stokes' law (Rogers and Yau 1989; Pruppacher and Klett 1997, 416). Stokes' law is $\overline{V}_w = g\left(\rho_r - \rho \right) D_w^2 / \left(18\rho\nu \right)$, which can be approximated as

$$\overline{V}_w = g\rho_r D_w^2 / \left(18\rho\nu \right). \tag{S13}$$

Therefore, no single equation predicts cloud water fall speeds over the entire range of cloud water diameters (2–100 μm). Regardless, the model was relatively insensitive to the equation that was used. Tests revealed a maximum difference of less than 1% (~0.5 m s^{-1}) in the maximum updraft speed for the Li50 case over 2 h. The diagnosed cloud droplet velocities using Eq. (S13) range from about 10^{-4} to 0.3 m s^{-1} near ground (T=20°C level) for simulated droplets of 2 to 100 μm, respectively.

In our simulations, we used the fall velocity equation for hexagonal-shaped rimed snow (Locatelli and Hobbs 1974) as an approximation for ice crystal fall velocities: $\overline{V_i} = cD_i^{\,d}\left(\rho_0/\rho\right)^{1/2}$. At very low temperatures, however, ice crystals may not rime nor aggregate and therefore the following hexagonal plate formulation may be more appropriate (from Pruppacher and Klett 1997):

$$\overline{V_i} = 58.51 D_i^{.824}\left(\rho_0/\rho\right)^{1/2}. \tag{S14}$$

This alternative formulation lessens the fall speeds of the smaller ice crystals and approaches snow-like velocities for the larger ice crystals. Sensitivity tests with the Li50 case reveal that either equation gives results that are very similar over a 2-hour simulation. Tests revealed a maximum relative difference of less than 1% in the maximum updraft speed between simulations with the two different $\overline{V_i}$ formulations. With Eq. (S14), the diagnosed ice crystal velocities range from about 0.003 to 0.6 m s^{-1} at an air density of 0.7565 kg m^{-3} for diameters 10 to 3000 μm, respectively.

4. Microphysical production terms

a. Autoconversion of cloud to rainwater

Autoconversion herein is the same as Orville and Kopp's (1977) derivation from Berry (1968) and is written as

$$\text{qrcnw} = \frac{\left(\rho 10^{-3}\right)\left\{\max\left[\left(q_w - q_{w,\text{crit}}\right), 0.0\right]\right\}^2}{\left[1.2x10^{-4} + \dfrac{1.596\times 10^{-18} N_w}{D_0\left(10^{-3}\rho\right)\left(q_w - q_{w,\text{crit}}\right)}\right]}. \tag{S15}$$

The number concentration of cloud droplets is represented by N_w and is set to 10^9 m^{-3} (constant). Cloud droplet dispersion is represented by D_0 and is set to 0.15 (constant). Notice that a "max" function is applied to insure that autoconversion will be zero unless q_w exceeds the threshold $q_{w,\text{crit}}$ of 2×10^{-3} kg kg^{-1}.

LFO83 noted that their simulated midlatitude storms seemed to exhibit a slower and more realistic precipitation development when qrcnw was switched off. We arbitrarily chose to retain qrcnw for the midlatitude simulations herein. Autoconversion is also included here for completeness since users may wish to use this microphysics scheme to simulate tropical warm-rain systems.

b. Sublimation and deposition (T_c<0°C)

1) SNOW AND HAIL/GRAUPEL

The following parameterizations are used to calculate vapor deposition/sublimation for snow and hail/graupel following LFO83. Negative values of Eqs. (S16) or (S17) indicate sublimation of snow or hail/graupel (positive qvsbs or qvsbh) and positive values indicate deposition (positive qsdpv or qhdpv). In the case of wet growth of hail/graupel, sublimation and deposition are turned off.

$$\text{qsdsv} = \left(\frac{2\pi}{\rho}\right)\left(S_i - 1\right)N_s \frac{\left[0.78\Gamma(2)D_{ns} + 0.308c^{1/2}S_c^{1/3}\nu^{-1/2}\Gamma\left(\dfrac{d+5}{2}\right)D_{ns}^{[d+3]/2}\left(\dfrac{\rho_0}{\rho}\right)^{1/4}\right]}{\left[\dfrac{L_s^2}{K_a R_v T^2} + \dfrac{1}{\rho q_{s,i}\psi}\right]}, \tag{S16}$$

$$\text{qhdsv} = \left(\frac{2\pi}{\rho}\right)\left(S_i - 1\right)N_h \frac{\left[0.78\Gamma(2)D_{nh} + 0.308\, S_c^{1/3}\nu^{-1/2}\Gamma(2.75)D_{nh}^{1.75}\left(\dfrac{4g\rho_h}{3C_d\rho}\right)^{1/4}\right]}{\left[\dfrac{L_s^2}{K_a R_v T^2} + \dfrac{1}{\rho q_{s,i}\psi}\right]}, \tag{S17}$$

$$\text{qvsbs} = \left|\min(\text{qsdsv},0)\right|, \tag{S18}$$

$$\text{qvsbh} = \left|\min(\text{qhdsv},0)\right|, \tag{S19}$$

$$\text{qsdpv} = \max(\text{qsdsv},0), \text{ and} \tag{S20}$$

$$\text{qhdpv} = \max(\text{qhdsv},0). \tag{S21}$$

2) CLOUD ICE (BERGERON PROCESS)

We follow the methodology of LFO83 who follow Hsie et al. (1980) and Koenig (1971) for estimating the Bergeron (deposition) growth of ice crystals into snow. Qsfw describes the rate at which cloud water produces snow by the Bergeron growth of ice crystals from 40 to 50 μm as well by riming 50 μm ice crystals, with radius

R_{I50} and terminal velocity V_{I50} via geometric sweep-out (from Hsie et al. 1980):

$$\text{qsfw} = N_{I50}\left[\frac{(.001)^{a_2}}{\rho}a_1 m_{I50}{}^{a_2} + E_{i,w}\pi R_{I50}^2 q_w V_{I50}\right]. \quad \text{(S22)}$$

The efficiency, $E_{i,w}$, of this accretion is assumed to be unity. The number concentration of 50 μm ice crystals is computed using,

$$N_{I50} = \frac{\rho q_i(\Delta t/\Delta t_1)}{m_{I50}}, \quad \text{(S23)}$$

where Δt is the model time step and Δt_1 is the empirically determined time for ice crystals to grow from 40 to 50 μm via the Bergeron process thereby increasing in mass from m_{I40} to m_{I50}.

TABLE S1. Temperature-dependent parameters, a_1 and a_2, used in computing the required time for 40 μm ice crystals to grow to 50 μm. Reprinted from Koenig (1971).

Temperature (°C)	a_1*	a_2
0	0.0000	0.0000
–1	0.7939E–7	0.4006
–2	0.7841E–6	0.4831
–3	0.3369E–5	0.5320
–4	0.4336E–5	0.5307
–5	0.5285E–5	0.5319
–6	0.3728E–5	0.5249
–7	0.1852E–5	0.4888
–8	0.2991E–6	0.3894
–9	0.4248E–6	0.4047
–10	0.7434E–6	0.4318
–11	0.1812E–5	0.4771
–12	0.4394E–5	0.5183
–13	0.9145E–5	0.5463
–14	0.1725E–4**	0.5651
–15	0.3348E–4	0.5813
–16	0.1725E–4	0.5655
–17	0.9175E–5	0.5478
–18	0.4412E–5	0.5203
–19	0.2252E–5	0.4906
–20	0.9115E–6	0.4447
–21	0.4876E–6	0.4126
–22	0.3473E–6	0.3960
–23	0.4758E–6	0.4149
–24	0.6306E–6	0.4320
–25	0.8573E–6	0.4506
–26	0.7868E–6	0.4483
–27	0.7192E–6	0.4460
–28	0.6513E–6	0.4433
–29	0.5956E–6	0.4413
–30	0.5333E–6	0.4382
–31	0.4834E–6	0.4361

*In the a_1 values, the exponent of 10 is shown after the E, e.g., 0.7939E–7 = 0.7939×10^{-7}.

**Note that a_1 appears as 0.1725E–6 in Koenig (1971) but this is a typographical error. The correct value shown in the table above was used in all of the final simulations presented in the main text. However, the correction had little noticeable impact on the solution. We thank the anonymous reviewer who brought this typographical error to our attention.

That time is defined as

$$\Delta t_1 = \frac{(.001)^{1-a_2}\left[m_{I50}^{(1-a_2)} - m_{I40}^{(1-a_2)}\right]}{a_1(1-a_2)}. \quad \text{(S24)}$$

The empirically determined temperature-dependent parameters, a_1 and a_2, from Koenig (1971), are presented in Table S1 to insure model result reproducibility. The model air temperature is converted to an integer when diagnosing a_1 and a_2.

Additionally, qsfi estimates the rate at which q_i is transformed to q_s via the Bergeron process and is presented as follows:

$$\text{qsfi} = q_i/\Delta t_1\,. \quad \text{(S25)}$$

c. Accretions

Three general equations describe accretion. The first involves an exponential Marshall-Palmer (EMP) distribution that accretes a monodisperse (MD) distribution (abbreviated, qx$_e$acy$_m$). The second involves an EMP distribution that accretes another EMP distribution (qx$_e$acy$_e$). The third involves a MD distribution that accretes a EMP distribution (qx$_m$acy$_e$). There are six types of qx$_e$acy$_m$ (qracw, qsacw, qhacw, qraci, qsaci, and qhaci), four types of qx$_e$acy$_e$ (qsacr, qracs, qhacr, and qhacs) and one type of qx$_m$acy$_m$ (qiacr) in the scheme.

1) DERIVING THE ACCRETION TENDENCIES

Our qx$_e$acy$_e$ accretion rates are the same as in Wisner et al. (1972) and LFO83. Our qx$_e$acy$_m$ and qx$_m$acy$_e$, however, differ from theirs. First, although they applied the following approximation in the derivation of qx$_e$acy$_e$, $\iint\left|V_x(D_x)-V_y(D_y)\right|dD_x dD_y = \left|\overline{V}_x-\overline{V}_y\right|\iint dD_x dD_y$, we additionally apply this approximation to qx$_e$acy$_m$ and qx$_m$acy$_e$ in order to retain the diameter and fall velocity of the MD species. [Note that Verlinde et al. (1990) found an analytic solution that would make this approximation unnecessary.] Because LFO83 and Wisner et al. (1972) neglected the MD species diameter and fall velocity, they were able to substitute the equation for *V(D)* for the EMP species prior to integration (of qx$_e$acy$_m$ and qx$_m$acy$_e$). These are the reasons for the derivation differences.

The impact of retaining *D* for the MD species is that substantially increased accretion rates can result compared to those in LFO83. This is especially true when the mean diameter of the EMP species is small and diameter of the MD species is large. Scale analysis reveals that these accretion rate increases are about two orders of magnitude greater when ice is involved since

D_i can be 100 times larger than D_w. However, the impact of subtracting a nonzero mass-weighted fall velocity for the MD species reduces the accretion rates slightly.

The derivation of qx_eacy_m (Eq. S29) and qx_eacy_e (Eq. S30) begins with Eqs. S26 and S27, which are identical to those, used by Wisner et al. (1972). The derivation of qx_macy_e (Eq. S31) begins with the expression in Eq. (S28) which is identical to that used by Rutledge and Hobbs (1984) except for a conversion of units.

The starting expressions of each derivation are written as

$$\text{qx}_e\text{acy}_m = \int \pi\left(\frac{D_{x_e}+D_{y_m}}{2}\right)^2 \left|V_{x_e}(D_{x_e}) - V_{y_m}(D_{y_m})\right| E_{x_e,y_m} q_{y_m} n_{x_e}(D_{x_e})dD_{x_e}, \quad \text{(S26)}$$

$$\text{qx}_e\text{acy}_e = \iint \pi\left(\frac{D_{x_e}+D_{y_e}}{2}\right)^2 \left|V_{x_e}(D_{x_e}) - V_{y_e}(D_{y_e})\right| E_{x_e,y_e}\left(\rho_{y_e}\frac{\pi D_{y_e}^3}{6}\right) n_{y_e}(D_{y_e})dD_{y_e} n_{x_e}(D_{x_e})dD_{x_e}, \quad \text{(S27)}$$

$$\begin{aligned}\text{qx}_m\text{acy}_e &= \frac{N_{x_m}}{\rho}\frac{dM_{x_m}}{dt} \\ &= \frac{N_{x_m}}{\rho}\int_0^\infty \pi\left(\frac{D_{x_m}+D_{y_e}}{2}\right)^2 \left|V_{x_m}(D_{x_m}) - V_{y_e}(D_{y_e})\right| E_{x_m,y_e}\left(\rho_{y_e}\frac{\pi D_{y_e}^3}{6}\right) n_{y_e}(D_{y_e})dD_{y_e},\end{aligned} \quad \text{(S28)}$$

and the derived expressions are

$$\text{qx}_e\text{acy}_m = \frac{\pi}{4} E_{x_e,y_m} N_{x_e} q_{y_m}\left|\overline{V}_{x_e} - \overline{V}_{y_m}\right| \left[\Gamma(3)D_{nx_e}^2 + 2\Gamma(2)D_{nx_e}^1 D_{y_m}^1 + \Gamma(1)D_{y_m}^2\right], \quad \text{(S29)}$$

$$\text{qx}_e\text{acy}_e = \frac{\pi}{4} E_{x_e,y_e} N_{x_e} q_{y_e}\left|\overline{V}_{x_e} - \overline{V}_{y_e}\right| \left[\frac{\Gamma(4)\Gamma(3)D_{nx_e}^2 + 2\Gamma(5)\Gamma(2)D_{nx_e}^1 D_{ny_e}^1 + \Gamma(6)\Gamma(1)D_{ny_e}^2}{\Gamma(4)}\right], \quad \text{(S30)}$$

$$\text{qx}_m\text{acy}_e = \frac{\pi}{4} E_{x_m,y_e} N_{x_m} q_{y_e}\left|\overline{V}_{x_m} - \overline{V}_{y_e}\right| \left[\frac{\Gamma(6)D_{ny_e}^2 + 2\Gamma(5)D_{ny_e}^1 D_{x_m}^1 + \Gamma(4)D_{x_m}^2}{\Gamma(4)}\right]. \quad \text{(S31)}$$

2) COLLECTION EFFICIENCIES

All collection efficiencies follow LFO83 and are assumed to be invariant with particle diameter. In most cases, an efficiency of unity is assumed ($E_{r,w}=1$, $E_{s,w}=1$, $E_{h,w}=1$, $E_{r,i}=1$, $E_{i,r}=1$, $E_{s,r}=1$, $E_{r,s}=1$, and $E_{h,r}=1$). However, for qhaci, qsaci, and qhacs, the following collection efficiencies are assumed:

$$E_{h,i} = \begin{cases} 0.1, & T < T_0 \\ 1.0, & \text{otherwise} \end{cases}, \quad \text{(S32)}$$

$$E_{s,i} = \exp\left[0.025 \min(T_c, 0)\right], \quad \text{(S33)}$$

$$E_{h,s} = \begin{cases} \exp\left[0.09\left(T - T_0\right)\right], & T < T_0 \\ 1.0, & \text{otherwise} \end{cases}. \quad \text{(S34)}$$

Future work is needed to test the model sensitivity to these assumed efficiencies.

3) THREE-COMPONENT ACCRETION PROCESS

In certain cases, accretions between two species contribute to a third species. Occurrence criteria are described below and are also presented in the budgets in supplemental section 4n. For simplicity, all three-component interactions here follow LFO83.

For warmer-than-freezing temperature:

- qsacw contributes to rain.

For subfreezing air temperature:

- qraci produces hail/graupel if rain exceeds 10^{-4} kg kg^{-1}. Otherwise qraci produces snow.
- qsacr and qracs both produce hail/graupel if snow or rain is greater than or equal to 10^{-4} kg kg^{-1}. Otherwise only qsacr is operative and it produces snow.
- qiacr produces hail/graupel if rain is greater than or equal to 10^{-4} kg kg^{-1}. Otherwise, qiacr produces snow.

For our higher shear cases (U_s = 50 m s^{-1}), we found that the microphysical structure was rather insensitive to factor-of-five changes in these mass thresholds. Ferrier (1994), however, found that changes in these thresholds did impact the microphysical storm structure.

d. Melting ($T_c > 0$°C)

Three types of melting processes exist in the microphysics scheme. All are applied in air temperatures above freezing. The first is the rate of increase in cloud water because of melting cloud ice (qwmli) which occurs completely in one step. The second and third (Eqs. S35 and S36) parameterize rain increases owing to melting snow and hail/graupel, respectively. These are quite similar to one another. They follow LFO83 except that they are written in terms of a gain for rain:

$$\text{qrmls} = -\min\left\{\begin{array}{l} -\dfrac{2\pi}{\rho L_f} N_s\left[K_a(T-T_0)+\rho\psi L_v\left(q_v-q_{s,0}\right)\right] \\ \times\left[0.78\Gamma(2)D_{ns}+0.308c^{1/2}S_c^{1/3}\nu^{-1/2}\Gamma\left(\dfrac{d+5}{2}\right)D_{ns}^{(d+3)/2}\left(\dfrac{\rho_0}{\rho}\right)^{1/4}\right] \\ -\dfrac{c_w(T-T_0)}{L_f}\left(\text{qsacw}+\text{qsacr}\right),0 \end{array}\right\}, \tag{S35}$$

$$\text{qrmlh} = -\min\left\{\begin{array}{l} -\dfrac{2\pi}{\rho L_f} N_h\left[K_a(T-T_0)+\rho\psi L_v\left(q_v-q_{s,0}\right)\right] \\ \times\left[0.78\Gamma(2)D_{nh}+0.308\,S_c^{1/3}\nu^{-1/2}\Gamma(2.75)D_{nh}^{1.75}\left(\dfrac{4g\rho_h}{3C_d\rho}\right)^{1/4}\right] \\ -\dfrac{c_w(T-T_0)}{L_f}\left(\text{qhacw}+\text{qhacr}\right),0 \end{array}\right\}. \tag{S36}$$

In the context of these equations, T_0 and $q_{s,0}$ refer to the particle state whereas T and q_v refer to the air state. Melting particles are assumed to maintain a surface temperature of 0°C until completely melted.

In these equations, the heat gained by conduction with dry, above-freezing air temperature can compete with the latent heat lost during evaporation. These melting formulations also include an approximation for the ice that is melted if that ice accretes above-freezing cloud water and rainwater (Wisner et al. 1972).

e. Evaporation of rain

The following rate of vapor production due to rainwater evaporation, active only in subsaturated air, is identical to LFO83 except the rate is written in terms of the vapor gain rather than the rain loss:

$$\text{qvevr} = -\left(\frac{2\pi}{\rho}\right)\min\left[(S-1),\ 0\right]N_r\,\frac{\left[0.78\Gamma(2)D_{nr}+0.308a^{1/2}S_c^{1/3}\nu^{-1/2}\Gamma\left(\dfrac{b+5}{2}\right)D_{nr}^{[b+3]/2}\left(\dfrac{\rho_0}{\rho}\right)^{1/4}\right]}{\left[\dfrac{L_v^2}{K_aR_vT^2}+\dfrac{1}{\rho q_{s,w}\psi}\right]}. \tag{S37}$$

f. Freezing

Two direct freezing processes exist in the microphysics. The first is homogeneous freezing of cloud water (T_c < –40°C) and the second is probabilistic freezing of rainwater (T_c < 0°C). The homogeneous freezing of cloud water to cloud ice (qifzw) occurs completely in one step. The probabilistic freezing of rainwater (from Bigg 1953) is parameterized as in LFO83:

$$\text{qhfzr} = 20\pi^2 B' N_r\left(\frac{\rho_w}{\rho}\right) \times\left(\exp\left\{\max\left[A'\left(T_0-T\right),0\right]\right\}-1\right)D_{nr}^6. \tag{S38}$$

In this equation, B' =100 m^{-3} s^{-1} and A' = 0.66 K^{-1}.

g. Aggregation

Aggregation rates of ice crystals forming snow and snow forming hail/graupel (both at T_c < 0°C) follow LFO83. The rate of aggregation of ice crystals and aggregation of snow may be written as

$$\text{qscni} = \alpha_1 \max\left[(q_i - q_{i,\text{crit}}),0\right], \qquad \text{(S39)}$$

$$\text{qhcns} = \alpha_2 \max\left[(q_s - q_{s,\text{crit}}),0\right], \qquad \text{(S40)}$$

respectively, where $\alpha_1 = 10^{-3}\exp\left[0.025\min\left(T_c,0\right)\right]$, $q_{i,\text{crit}} = 1\times10^{-3}$ kg kg^{-1}, $\alpha_2 = 10^{-3}\exp\left[0.09\left(T - T_0\right)\right]$, and $q_{s,\text{crit}} = 6\times10^{-4}$ kg kg^{-1}.

These aggregation rates are crude since they do not include particle diameter and riming criteria. For instance, hexagonal plates should probably not aggregate into snow until their diameters exceed 300–450 μm (Pruppacher and Klett 1978). Also, snow should probably not aggregate into hail/graupel unless sufficient riming occurs.

h. Rain droplet shedding by hail/graupel

Before shedding can be computed, hail/graupel growth is diagnosed as either wet or dry. As in LFO83 the smaller of qhdry and qhwet is used to represent the actual growth rate since qhwet is derived assuming maximized wet growth conditions. Only dry growth is allowed at temperatures colder than –40°C. The dry and wet growth rates are written following LFO83:

$$\text{qhdry} = \text{qhacr} + \text{qhacw} + \text{qhaci} + \text{qhacs}, \qquad \text{(S41)}$$

$$\text{qhwet} = \max\left\{\begin{array}{l} -\dfrac{2\pi}{\rho\left[L_f + c_w(T-T_0)\right]} N_h\left[K_a(T-T_0) + \rho\psi L_v\left(q_v - q_{s,0}\right)\right] \\ \times\left[0.78\Gamma(2)D_{nh} + 0.308\, S_c^{1/3}\nu^{-1/2}\Gamma(2.75)D_{nh}^{1.75}\left(\dfrac{4g\rho_h}{3C_d\rho}\right)^{1/4}\right] \\ +\left[1 - \dfrac{c_i(T-T_0)}{L_f + c_w(T-T_0)}\right]\left(\text{qhaci} + \text{qhacs}\right), 0 \end{array}\right\}. \qquad \text{(S42)}$$

Although not mentioned by LFO83, one needs to apply the "max" function to prevent negative qhwet due to a singularity that can occur at low temperatures. As in LFO83, for the case of wet growth, qhaci and qhacs are recomputed assuming efficiencies of 1.0 instead of the efficiencies reported earlier. As in the case of qrmlh, this equation assumes a 0°C particle temperature for wet hail/graupel.

The rain frozen or shed from hail/graupel undergoing wet growth at temperatures cooler than freezing is

$$\text{qrshh} = -\text{qhwet} + (\text{qhacr} + \text{qhacw}). \qquad \text{(S43)}$$

Although they do not use an explicit shedding term, analysis of the resulting water budgets in Hsie et al. (1980) and Orville and Kopp (1977) shows that the effect of qrshh is the same. That is, positive values of qrshh indicate the rate that rain is acquired due to hail/graupel shedding because the accretion of rain and cloud water exceeds that required for wet growth. Negative values of qrshh indicate the rate that rain freezes onto hail/graupel because the accretion of rain and cloud water is less than required for wet growth conditions.

At temperatures warming than freezing, hail/graupel sheds any accretions as rain:

$$\text{qrshh} = [\text{qhacr} + \text{qhacw} + \text{qhaci} + \text{qhacs}]. \qquad \text{(S44)}$$

Substituting qrshh from Eqs. (S43) or (S44) into the budget in supplemental section 4n reveals this shedding behavior more clearly.

i. Ice crystal initiation

At temperatures below freezing and only in supersaturated air with respect to ice (S_i> 1), new cloud ice mixing ratio is produced via the lesser of the following two values:

$$\text{qiint} = \frac{1}{\Delta t}\min\left[\frac{M_{i0}N_{in}}{\rho_0}, \frac{\left(S_i - 1\right)}{\left(1 + \dfrac{L_v^2 q_{s,i}}{c_p R_v T^2}\right)}\right]. \qquad \text{(S45)}$$

The procedure and formula are similar to RH83 and Stephens (1979). The number concentration of active ice nuclei is given by N_i, defined previously, with an assumed starting mass (M_{i0}) of 10^{-12} kg for each nucleated ice crystal. The second value in the formula is provided as a safeguard to prevent the first value in the formula from exceeding the amount of available water vapor (RH83).

j. Saturation adjustment

We use a saturation adjustment scheme nearly identical to that presented by Tao et al. (1989) because, when the ice species are removed, it reduces to the liquid-only saturation adjustment scheme used by Soong and Ogura (1973) and Klemp and Wilhelmson (1978). In 1988, J. M. Straka derived this saturation adjustment procedure and it will be presented in a forthcoming paper for multiple ice habits.

The saturation adjustment procedure includes the following six processes: condensation and evaporation of cloud water (qwcdv & qvevw), deposition and sublimation of cloud ice (qidpv & qvsbi), and melting and homogeneous freezing of cloud ice (qwmli & qifzw). Melting and homogeneous freezing of cloud ice occur first. Then saturation is diagnosed. For supersaturated conditions, qwcdv and qidpv are calculated to remove any supersaturated vapor. For subsaturated conditions in the presence of q_w and q_i, qvevw and qvsbi are calculated to remove the subsaturation. We iterated the implicit saturation adjustment scheme twice in an attempt to produce a closer solution to the linearized version of Tetens' formula. However, experiments made after the fact show that this is not necessary. See Tao et al. (1989) for further details.

k. Prevention of spurious growth

Minimum mixing ratio thresholds are required in order to activate nearly all microphysics processes described herein. These minimum mixing ratio criteria are as follows: q_w=10^{-9}, q_i=10^{-12}, q_r=10^{-7}, q_s=10^{-7}, and q_h=10^{-7} kg kg^{-1}. For example, q_s must exceed 10^{-7} kg kg^{-1} before it is allowed to grow via deposition or aggregate into hail/graupel. As another example, respective minimum mass thresholds are required prior to accretion of species *y* by species *x*. Our experience is that these minimum mixing ratio criteria are, on the Cray J90, sufficient for preventing growth of spurious mixing ratio caused by "overshoots" in the numerical filtering and truncation error. Others such as Proctor (1987) perform a similar procedure to prevent such "numerical seeding" of the microphysics.

l. Numerical stability of the microphysics

We limit nearly all of the above microphysics tendencies to remove no more than 20% of the source mixing ratio per time step in order to insure numerical stability. One may think of this stability constraint as a Courant number (Courant et al. 1928) for the microphysics. Although Ferrier (1994) notes that such a constraint is rarely needed except in the case of ice accreting rain (qiacr), this constraint is consistently applied to all tendencies except for those that would either need to occur completely in a single time step or would rarely violate the Courant condition. For instance homogeneous freezing of cloud drops (qifzw) and homogeneous melting of cloud ice (qwmli) need to occur completely in one time step. Also, the deposition of vapor onto hail/graupel or snow is not constrained since presumably updrafts would rarely be lacking in water vapor. Also, the 20% constraint is not needed in the initiation of cloud ice since the formulation already includes a constraint.

m. Miscellaneous variables

The following section provides definitions for the following variables: specific heat of ice at constant pressure (c_i); diffusivity of water vapor (ψ) in air;

TABLE S2. Microphysics species and source & sink rates used in the simple liquid/ice microphysics scheme. Sources and sinks in bold typeface are handled last as part of the saturation adjustment scheme. Boolean operators are zero unless the following is true: δ_D = 1 if q_h is undergoing dry growth, δ_f = 1 if T_c < 0°C, δ_H = 1 if T_c < –40°C, δ_r = 1 if q_r < 10^{-4} kg kg^{-1}, and δ_s = 1 if q_s < 10^{-4} kg kg^{-1}.

Species	Sources	Sinks
Vapor (q_v)	qvevr + **qvevw** + δ_f [δ_D (qvsbh + qvsbs) + **qvsbi**]	δ_f [– qiint – **qidpv** + δ_D (–qhdpv –qsdpv)] – **qwcdv**
Cloud water (q_w)	**qwcdv** + (1–δ_f) **qwmli**	–qracw – qrcnw – qsacw – qhacw – **qvevw** –δ_f qsfw –δ_H **qifzw**
Rain (q_r)	qracw + qrcnw + qrshh+ (1–δ_f)(qsacw + qrmlh + qrmls)	–qvevr – qhacr + δ_f (– qiacr – qhfzr – qsacr)
Cloud ice (q_i)	δ_f (qiint + **qidpv**) + δ_H (**qifzw**)	δ_f (–qscni – qsaci – qraci – qsfi – **qvsbi**) – (1–δ_f) **qwmli** – qhaci
Snow (q_s)	δ_f [qsacw + qscni + qsaci + qsfi + qsfw + δ_r (qraci + qiacr) + $\delta_s \delta_r$ (qsacr) + δ_D qsdpv]	– qhcns – qhacs –(1–δ_f) qrmls +δ_f [–δ_D qvsbs – (1– $\delta_s \delta_r$) qracs]
Hail/ graupel (q_h)	qhacr + qhacw + qhacs + qhaci + qhcns +δ_f [qhfzr + δ_D qhdpv +(1–δ_r)(qraci + qiacr) + (1– $\delta_s \delta_r$)(qsacr + qracs)]	– qrshh – (1–δ_f)qrmlh – ($\delta_f \delta_D$) qvsbh

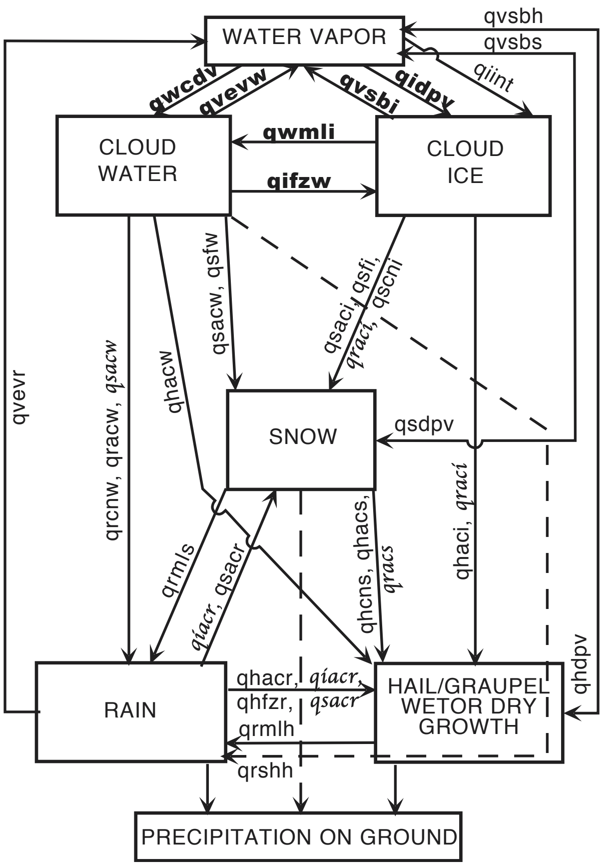

FIG. S1. Visual depiction of the microphysical transfer rates between water species. Arrows point toward (away from) the species that experiences the gain (loss). Three-component processes are labeled in script. Processes within saturation adjustment are labeled in bold. Adapted from LFO83.

thermal conductivity (K_a) and kinematic viscosity (ν) of air; and Schmidt number (S_c). Formulas for c_i and ψ are taken from pages 89 and 413 of Pruppacher and Klett (1978), respectively. The respective formulas for K_a and ν are from Wisner et al. (1972) and List (1984):

$$c_i = 10^3\left[2.118636 + 0.007371(T - T_0)\right], \tag{S46}$$

$$\psi = 2.11\times10^{-5}\left(\frac{101325}{p}\right)\left(\frac{T}{T_0}\right)^{1.94}, \tag{S47}$$

$$K_a = 2.43\times10^{-2}\left(\frac{\rho\nu}{1.718\times10^{-5}}\right), \tag{S48}$$

$$\nu = \frac{1.832\times10^{-5}}{\rho}\left(\frac{296.16+120}{T+120}\right)\left(\frac{T}{296.16}\right)^{1.5}, \tag{S49}$$

$$S_c = \nu/\psi \tag{S50}$$

n. Net production and loss for each species

Table S2 and Fig. S1 and show the source and sink rates for each species. The net sum for each species gives the rate of change in species mixing ratio per time step. The sum of all species sources and sinks is zero. Boolean operators δ_D, δ_f, δ_H, δ_r, and δ_s have the purpose of turning processes on or off depending upon the microphysical and state conditions. For instance, δ_f is switched on for cooler-than-freezing conditions and off for warmer conditions. These Boolean operators are also important for regulating the three-component accretion process described in section 4c3.

o. Liquid-only version

All ice processes are turned off for the liquid-only version. The only remaining processes (P in Eq. S1) are rainwater evaporation, autoconversion, and accretion of cloud droplets by rain (qvevr, qracw, and qrcnw). Of course, cloud water condensation (qwcdv) and evaporation (qvevw) are included within the saturation adjustment procedure.

SUPPLEMENTAL APPENDIX

List of Symbols

Notation	Description	Value	SI units
a	Constant in the fallspeed relation for rain and cloud water	841.99666	$m^{(1-b)} s^{-1}$
A'	Constant in Bigg raindrop freezing equation	0.66	K^{-1}
$a1, a2$	Temperature-dependent parameters in the Bergeron process		
b	Constant in fallspeed relation for rain and cloud water	0.8	
B'	Constant in Bigg raindrop freezing equation	100	$m^{-3} s^{-1}$
c	Constant in fallspeed relation for snow and cloud ice	4.83607122	$m^{(1-d)} s^{-1}$
ccn_w	Cloud condensation nuclei number per volume (a.k.a., N_w)	10^9	m^{-3}

SUPPLEMENTAL APPENDIX (*Continued*)

Notation	Description	Value	SI units
C_D	Drag coefficient for hail/graupel	1.0 ($\rho_h < 600$) 0.6 ($\rho_h \geq 600$)	No dim.
c_i	Specific heat of ice at constant pressure	(Eq. S46)	J kg^{-1} K^{-1}
c_p	Specific heat of dry air at constant pressure	1004	J kg^{-1} K^{-1}
c_w	Specific heat of liquid water at constant pressure	4218	J kg^{-1} K^{-1}
d	Constant in fallspeed relation for snow and cloud ice	0.25	
D	Subscript used to indicate dry growth of q_h		
D_0	Dispersion in distribution of cloud water droplets (used in autoconversion)	0.15	No dim.
D_i	Particle diameter of monodisperse ice crystals	(Eq. S7)	m
D_{nx}	Mean particle diameter of species distribution x (Includes D_{nr}, D_{ns}, and D_{nh})	(Eq. S3)	m
D_w	Particle diameter of monodisperse cloud droplets	(Eq. S5)	m
D_x, D_y	Particle diameter of species x or y (where x or $y = w, r, i, s, or\ h$)		m
e	Subscript used to indicate a Marshall–Palmer exponential distribution for species x or y.		
$E_{x,y}$	Efficiency of species x collecting species y ($E_{h,r}$, $E_{h,s}$, $E_{h,w}$, $E_{i,r}$, $E_{i,w}$, $E_{r,i}$, $E_{r,s}$, $E_{r,w}$, $E_{s,i}$, $E_{s,r}$, $E_{s,w}$)		No dim.
f	Subscript indicating freezing conditions ($T_c < 0°C$)		
g	Gravitational constant	9.8	m s^{-2}
h	Hail/graupel subscript		
H	Subscript indicating homogeneous freezing conditions ($T_c < -40°C$)		
i	Cartesian directions (i =1, 2, 3)		
i	Cloud ice species subscript		J kg^{-1} K^{-1}
K_a	Thermal conductivity of air	(Eq. S48)	J m^{-1}s^{-1} K^{-1}
K_h	Eddy mixing coefficient		m^2 s^{-1}
L_f	Latent heat of fusion	335 717.	J kg^{-1}
L_s	Latent heat of sublimation	2 836 017.	J kg^{-1}
L_v	Latent heat of vaporization	2 500 300.	J kg^{-1}
m	Subscript used to indicate a monodisperse distribution in species x or y		
M_i	Mass of a single cloud ice particle	(Eq. S8)	kg
M_{i0}	Starting mass of a newly-initiated cloud ice particle	10^{-12}	kg
m_{I40}	Mass of a 40 μm radius ice crystal (used in the Bergeron process)	2.4546×10^{-10}	kg
m_{I50}	Mass of a 50 μm radius ice crystal (used in the Bergeron process)	4.8×10^{-10}	kg
M_w	Mass of a single cloud droplet	(Eq. S6)	kg
M_x	Mass of a single particle from a general monodisperse distribution of species x		kg
N_h	Number concentration of hail/graupel	$n_{oh}\, D_{nh}$	m^{-3}
N_i	Number concentration of cloud ice crystals	(Eq. S9)	m^{-3}
N_{I50}	Number concentration of hypothetical 50 μm radius ice crystals (Bergeron)	(Eq. S23)	kg^{-1}
N_{in}	Number concentration of active natural ice nuclei	(Eq. S9)	m^{-3}
N_{in0}	Number concentration of active natural ice nuclei as T→ 0°C	0.01	m^{-3}
n_{oh}	Intercept parameter for hail/graupel	4×10^4	m^{-4}
n_{or}	Intercept parameter for rain	8×10^6	m^{-4}
n_{os}	Intercept parameter for snow	3×10^6	m^{-4}
n_{ox}	Intercept parameter for species x (where $x = r, s,$ or h)		m^{-4}
N_r	Number concentration of rain	$n_{or}\, D_{nr}$	m^{-3}
N_s	Number concentration of snow	$n_{os}\, D_{ns}$	m^{-3}
N_w	Number concentration of activated cloud droplets	10^9	m^{-3}
N_x	Number concentration of species x having a Marshall–Palmer exponential distribution	(Eq. S4)	m^{-3}
$n_x(D_x)$	Number concentration per diameter size for species x having a Marshall–Palmer exponential distribution	(Eq. S2)	m^{-4}
P	Variable representing the sum of the microphysical source and sink rates for a species.		kg kg^{-1} s^{-1}
qhcns	Production rate of q_h via q_s aggregation	(Eq. S40)	kg kg^{-1} s^{-1}
qhdpv	Production rate of q_h via deposition of q_v	(Eq. S21)	kg kg^{-1} s^{-1}
qhdry	Production rate of q_h assuming dry growth.	(Eq. S41)	kg kg^{-1} s^{-1}
qhdsv	Deposition/Sublimation calculation for q_h	(Eq. S17)	kg kg^{-1} s^{-1}
qhfzr	Production rate of q_h via Bigg (probabilistic) freezing of q_r	(Eq. S38)	kg kg^{-1} s^{-1}
qhwet	Production rate of q_h assuming maximum possible wet growth	(Eq. S42)	kg kg^{-1} s^{-1}
$q_{i,\mathrm{crit}}$	Critical threshold for cloud ice aggregation	1×10^{-3}	kg kg^{-1}
qidpv	Production rate of q_i via deposition of q_v	Section 4j	kg kg^{-1} s^{-1}
qifzw	Production rate of q_i via homogeneous freezing of q_w	Section 4j	kg kg^{-1} s^{-1}
qiint	Production rate of q_i via initiation	(Eq. S45)	kg kg^{-1} s^{-1}
q	Mixing ratio of species (Possibilities include q_v, q_w, q_r, q_i, q_s, and q_h)		kg kg^{-1}
qrcnw	Production rate of q_r via autoconversion of q_w	(Eq. S15)	kg kg^{-1} s^{-1}

SUPPLEMENTAL APPENDIX (*Continued*)

Notation	Description	Value	SI units
qrmlh	Production rate of q_r via melting of q_h	(Eq. S36)	$kg\,kg^{-1}\,s^{-1}$
qrmls	Production rate of q_r via melting of q_s	(Eq. S35)	$kg\,kg^{-1}\,s^{-1}$
qrshh	Production rate of q_r via shedding of q_h	(Eqs. S43–S44)	$kg\,kg^{-1}\,s^{-1}$
$q_{s,0}$	Saturation mixing ratio for water vapor at a hail/graupel surface		$kg\,kg^{-1}$
$q_{s,\text{crit}}$	Critical threshold for snow aggregation	6×10^{-4}	$kg\,kg^{-1}$
$q_{s,i}$	Saturation mixing ratio for water vapor with respect to ice		$kg\,kg^{-1}$
$q_{s,w}$	Saturation mixing ratio for water vapor with respect to liquid water		$kg\,kg^{-1}$
qscni	Production rate of q_s via q_i aggregation	(Eq. S39)	$kg\,kg^{-1}\,s^{-1}$
qsdpv	Production rate of q_s via deposition of q_v	(Eq. S20)	$kg\,kg^{-1}\,s^{-1}$
qsdsv	Deposition/Sublimation calculation for q_s	(Eq. S16)	$kg\,kg^{-1}\,s^{-1}$
qsfi	Production rate of q_s via Bergeron growth of q_i	(Eq. S25)	$kg\,kg^{-1}\,s^{-1}$
qsfw	Production rate of q_s via Bergeron transfer from q_w	(Eq. S22)	$kg\,kg^{-1}\,s^{-1}$
qvevr	Production rate of q_v via evaporation of q_r	(Eq. S37)	$kg\,kg^{-1}\,s^{-1}$
qvevw	Production rate of q_v via evaporation of q_w	Section 4j	$kg\,kg^{-1}\,s^{-1}$
qvsbh	Production rate of q_v via sublimation of q_h	(Eq. S19)	$kg\,kg^{-1}\,s^{-1}$
qvsbi	Production rate of q_v via sublimation of q_i	Section 4j	$kg\,kg^{-1}\,s^{-1}$
qvsbs	Production rate of q_v via sublimation of q_s	(Eq. S18)	$kg\,kg^{-1}\,s^{-1}$
$q_{w,\text{crit}}$	Critical threshold for cloud water coalescence	2×10^{-3}	$kg\,kg^{-1}$
qwcdv	Production rate of q_w via condensation of q_v	Section 4j	$kg\,kg^{-1}\,s^{-1}$
qwmli	Production rate of q_w via melting of q_i	Section 4j	$kg\,kg^{-1}\,s^{-1}$
q_x, q_y	Mixing ratio of general species *x* or *y* (Possibilities include q_v, q_w, q_r, q_i, q_s, and q_h)		$kg\,kg^{-1}$
qx$_e$acy$_e$	Production rate of species x_e due to accretion of species y_e. Includes qsacr, qracs, qhacr, and qhacs.	(Eqs. S27, S30)	$kg\,kg^{-1}\,s^{-1}$
qx$_e$acy$_m$	Production rate of species x_e (a Marshall–Palmer exponential distribution) due to accretion of species y_m (a monodisperse distribution). Includes qracw, qsacw, qhacw, qraci, qsaci, and qhaci.	(Eqs. S26, S29)	$kg\,kg^{-1}\,s^{-1}$
qx$_m$acy$_e$	Production rate of species x_m due to accretion of species y_e. Includes qiacr.	(Eqs. S28, S31)	$kg\,kg^{-1}\,s^{-1}$
r	Rain species subscript.		
R_{I50}	Ice crystal radius of 50 μm (for Bergeron process).	50×10^{-6}	m
R_v	Gas constant for water vapor.	461.5	$J\,kg^{-1}\,K^{-1}$
s	Snow species subscript		
S	Saturation ratio with respect to liquid		No dim.
S_c	Schmidt number	(Eq. S50)	No dim.
S_i	Saturation ratio with respect to ice		No dim.
t	Time		s
T	Temperature		K
T_c	Temperature		°C
T_o	Freezing/melting temperature	273.15	K
u_i	Velocity component in the three Cartesian directions (i =1, 2, or 3)		$m\,s^{-1}$
v	Water vapor species subscript		
V_{I50}	Terminal velocity of a 50 μm radius ice crystal (for Bergeron process)	1	$m\,s^{-1}$
$\overline{V}_x$	Mass-weighted mean terminal velocity for all particles in species *x*. Includes $\overline{V}_w, \overline{V}_r, \overline{V}_i, \overline{V}_s, \overline{V}_h$.	(Eqs. S10–S14)	$m\,s^{-1}$
$V_x(D_x)$	Terminal velocity for a single particle of diameter, *D*, within species *x* (where *x*=*w, r, i, s, or h*)		$m\,s^{-1}$
w	Cloud water species subscript		
x, y	General variables used to distinguish between different species		
x_3	Distance in the vertical direction		m
x_e	Exponential distribution species that is accreting.		
x_i	Distance in the three Cartesian directions (i =1, 2, or 3)		m
x_m	Monodisperse distribution species that is accreting		
y_e	Exponential distribution species being accreted.		
y_m	Monodisperse distribution species being accreted.		
α_1	factor in aggregation of ice		
α_2	factor in aggregation of snow		
β	Parameter used in Fletcher's formula	0.6	K^{-1}
δ_D	Boolean operator indicating dry hail/graupel growth	1 or 0	
δ_f	Boolean operator indicating whether $T_c <$ 0°C	1 or 0	

SUPPLEMENTAL APPENDIX (*Continued*)

Notation	Description	Value	SI units
δ_H	Boolean operator indicating whether T_c <–40°C	1 or 0	
δ_r	Boolean operator indicating whether $q_r < 10^{-4}$ kg kg^{-1}	1 or 0	
δ_s	Boolean operator indicating whether $q_s < 10^{-4}$ kg kg^{-1}	1 or 0	
Δt	Change in time		s
Δt_1	Time required for an ice crystal to increase from 40 to 50 μm.	(Eq. S24)	s
Γ	gamma function		
ν	kinematic viscosity of air	(Eq. S49)	m^2 s^{-1}
π	Half of one revolution	3.1415927	Radians
ρ	Air density (of reference sounding)		kg m^{-3}
ρ_0	Reference air density	1.225	kg m^{-3}
ρ_h	Water density of hail/graupel	900	kg m^{-3}
ρ_r , ρ_w	Water density of rain or cloud water	1000	kg m^{-3}
ρ_s	Water density of snow	100	kg m^{-3}
ψ	diffusivity of water vapor in air	(Eq. S47)	m^2 s^{-1}

SUPPLEMENTAL REFERENCES

Berry, E. X., 1968: Modification of the warm rain process. Preprints, *1st Natl. Conf. on Weather Modification*, Albany, NY, Amer. Meteor. Soc., 81–88.

Bigg, E. K., 1953: The supercooling of water. *Proc. Phys. Soc. London*, **B66,** 688–694.

Chang, C.-H., 1977: Ice generation in clouds. M.S. thesis, South Dakota School of Mines and Technology, 129 pp. [Available from Devereaux Library, SDSM-T, 501 E. St. Joseph, Rapid City, SD 57701.]

Courant, R., K. O. Friedrichs, and H. Lewy, 1928: On the partial difference equations of the heat-conduction type. *Proc. Cambridge Philos. Soc*., **43,** 50–67.

Davis, C. I., and A. H. Auer, 1974: Use of isolated clouds to establish the accuracy of diffusional ice crystal growth. Proc. *Cloud Physics Conf.,* Tucson, AZ, Amer. Meteor. Soc., 141–147.

Ferrier, B. S., 1994: A double-moment multiple-phase four-class bulk ice scheme. Part I: Description. *J. Atmos. Sci.,* **51,** 249–280.

Fletcher, N. H., 1962: *The physics of rain clouds*. Cambridge University Press, 390 pp.

Gunn, R., and G. D. Kinzer, 1949: The terminal velocity of fall for water drops in stagnant air. *J. Meteor*., **6,** 243–248.

Hsie, E. Y., R. D. Farley, and H. D. Orville, 1980: Numerical simulation of ice-phase convective cloud seeding. *J. Appl. Meteor.,* **19,** 950–977.

Klemp, J. B., and R. B. Wilhelmson, 1978: The simulation of three-dimensional convective storm dynamics. *J. Atmos. Sci*., **35,** 1070–1096.

Koenig, L. R., 1971: Numerical modeling of ice deposition. *J. Atmos. Sci.,* **28,** 226–237.

Liu, J. Y., and H. D. Orville, 1969: Numerical modeling of precipitation and cloud shadow effects on mountain-induced cumuli. *J. Atmos. Sci*., **26,** 1283–1298.

Lin, Y.-L., R. D. Farley, and H. D. Orville, 1983: Bulk parameterization of the snow field in a cloud model. *J. Climate Appl. Meteor*., **22,** 1065–1092.

List, R., 1984: *Smithsonian Meteorological Tables*. Sixth Revised Edition. Smithsonian Institution Press, Washington D.C., 527 pp.

Locatelli, J. D., and P. V. Hobbs, 1974: Fall speeds and masses of solid precipitation particles. *J. Geophys Res*., **79,** 2185–2197.

Marshall, J. S., and W. M. Palmer, 1948: The distribution of raindrops with size. *J. Meteor*., **5,** 165–166.

Ogura, Y., and T. Takahashi, 1971: Numerical simulation of the life cycle of a thunderstorm cell. *Mon. Wea. Rev*., **99,** 895–911.

Orville, H. D., and F. J. Kopp, 1977: Numerical simulation of the history of a hailstorm. *J. Atmos. Sci.,* **34,** 1596–1618.

Proctor, F. H., 1987: The Terminal Area Simulation System. Vol. 1: Theoretical formulation. NASA Contractor Rep. 4046, NASA, Washington, DC, 176 pp. [Available from National Technical Information Service, Springfield, VA 22161.]

Pruppacher, H. R., and J. D. Klett, 1978: *Microphysics of Clouds and Precipitation*. D. Reidel, 714 pp.

——, and ——, 1997: *Microphysics of Clouds and Precipitation*. Kluwer Academic, 954 pp.

Rogers, R. R., and M. K. Yau, 1989: *A Short Course in Cloud Physics*. 3rd ed. Pergamon Press, 293 pp.

Rutledge, S. A., and P. V. Hobbs, 1983: The mesoscale and microscale organization of clouds and precipitation in midlatitude cyclones. VIII: A model for the "seeder-feeder" process in warm-frontal rainbands. *J. Atmos. Sci*., **40,** 1185–1206.

——, and ——, 1984: The mesoscale and microscale organization of clouds and precipitation in midlatitude cyclones. XII: A diagnostic modelling study of precipitation development in narrow cold-frontal rainbands. *J. Atmos. Sci*., **41,** 2949–2972.

Soong, S.-T., and Y. Ogura, 1973: A comparison between axisymmetric and slab-symmetric cumulus cloud models. *J. Atmos. Sci*., **30,** 879–893.

Stephens, M. A., 1979: A simple ice phase parameterization. Atmospheric Science Paper 319. M.S. thesis. Colorado State University, 122 pp. [Available from Morgan Library, 501 University Avenue, Fort Collins, CO 80523.]

Tao, W.-K., J. Simpson, and M. McCumber, 1989: Ice-water saturation adjustment. *Mon. Wea. Rev*., **117,** 231–235.

Verlinde, J., P. J. Flatau, and W. R. Cotton, 1990: Analytical solutions to the collection growth equation: Comparison with approximate methods and application to cloud microphysics parameterization schemes. *J. Atmos. Sci*., **47,** 2871–2880.

Wisner, C., H. D. Orville, and C. Myers, 1972: A numerical model of a hail-bearing cloud. *J. Atmos. Sci.,* **29,** 1160–1181.